Polymer Degradation and Stability 96 (2011) 1194–1203

Contents lists available at ScienceDirect

Polymer Degradation and Stability

journal homepage: www.elsevier.com/locate/polydegstab

The hydrolytic effect of moisture and hygrothermal aging on poly(butylene succinate)/organo-montmorillonite nanocomposites

Y.J. Phua, W.S. Chow, Z.A. Mohd Ishak*

School of Materials and Mineral Resources Engineering, Universiti Sains Malaysia, Engineering Campus, 14300 Nibong Tebal, Pulau Pinang, Malaysia

ARTICLE INFO

Article history:
Received 19 February 2011
Accepted 25 April 2011
Available online 1 May 2011

Keywords:
Hydrolysis
Moisture absorption
Hygrothermal aging
Poly(butylene succinate)
Nanocomposites
Biodegradable

ABSTRACT

The study of hydrolysis on biodegradable poly(butylene succinate) (PBS) is essential to predict the materials properties in a humid environment. In this study, PBS nanocomposites were exposed to different conditions of relative humidity (RH) and temperature. The moisture uptake increased with organo-montmorillonite (OMMT) loading and the RH of the testing environment. The exposure of PBS and the nanocomposites to a humid environment caused changes in the mechanical properties. The hydrolytic degradation becomes more pronounced upon hygrothermal aging at high temperature, whereby premature failure occurred. PBS nanocomposites were found to exhibit a better hydrolytic stability than neat PBS. The degradation was evaluated through Fourier transform infrared (FTIR) spectroscopy and gel permeation chromatography (GPC). A drastic reduction in the molecular weight of PBS has revealed the occurrence of degradation after exposure to moisture and heat. This has led to an alteration of the thermal behavior as investigated using differential scanning calorimetry (DSC).

1. Introduction

In recent years, much attention has been directed to biodegradable polymers because of their potential to minimize the environmental problems associated with the disposal of synthetic, non-biodegradable polymers. The substitution of these synthetic polymers with biodegradable polymers has become a great field of interest. Poly(butylene succinate) (PBS) is a synthetic aliphatic polyester with superior properties such as biodegradability, melt-processability and chemical stability [1–3]. PBS can be blended with organo-montmorillonite (OMMT) to form a nanocomposite with the intention of obtaining materials with improved properties suitable for a wide range of applications. The formation of a nanocomposite enables improvements in the thermal, mechanical, and flame retardant properties as well as dimensional stability [4–7].

PBS, a polyester, is susceptible to hydrolysis when exposed to moisture. Biodegradation of PBS normally initiated through the hydrolysis of ester linkages along the main polymer chain, subsequently leads to a reduction in molecular weight [8,9]. This process is affected by several factors such as moisture content, temperature and pressure of the environment. The hydrolysis process is generally accelerated by high moisture content and temperature. The combined effects of moisture and temperature on the materials are normally studied through the hygrothermal aging process. Moisture absorption and hygrothermal aging of polymers results in a detrimental effects on the mechanical, chemical, physical and degradability properties [10,11]. According to Mohd Ishak and Berry [12], hygrothermal aging can result in the degradation of polyesters both chemically and physically. Therefore, the study of hydrolytic properties of biodegradable PBS is of particular importance to estimating not only the influence of moisture and temperature on the material properties but also the degradability of PBS.

Numerous researchers have reported on the biodegradability of PBS under various conditions [13–15]. However, studies in the literature on the hydrolytic behavior of PBS are still very limited, even though hydrolysis is understood to be the primary process by which biodegradation starts. Because hydrolysis is a critical phenomenon for PBS, this paper reports on the moisture absorption and hygrothermal aging of PBS and its nanocomposites. Focus is also given to the effects of moisture content, OMMT loading and temperature on the hydrolysis of the nanocomposites. In previous studies, the effects of relative humidity (RH) and OMMT loading on the kinetics of moisture absorption have been reported [6]. Hence, this paper provides more intensive research on the effects of moisture and temperature to the mechanical properties and degradation. An investigation of the thermal behavior is compelling because such studies are rarely reported by researchers. In short, hydrolysis studies are vital for understanding biodegradable PBS nanocomposites in order to predict their life-time and possible applications in a humid environment.

* Corresponding author. Tel.: +60 4 5995999; fax: +60 4 5941011.
E-mail addresses: zarifin@eng.usm.my, zarifin.ishak@gmail.com (Z.A. Mohd Ishak).

0141-3910/$ – see front matter © 2011 Elsevier Ltd. All rights reserved.
doi:10.1016/j.polymdegradstab.2011.04.017

2. Experimental

2.1. Materials

PBS (Bionolle #1020) with a melting temperature of 115 °C and a density of 1.26 g/cm^3 was obtained from Showa Highpolymer Co., Ltd., Tokyo. OMMT (Nanomer® I.30 TC, cation exchange capacity, CEC = 110 mequiv/100 g) was supplied by Nanocor Inc., USA. It contained 70% montmorillonite (MMT) and 30% octadecylamine (ODA).

2.2. Preparation of nanocomposites

PBS was incorporated with various OMMT loadings (i.e., 2, 4, 6, 8 and 10 wt%) to form nanocomposites. First, PBS pellets and OMMT were dried in a vacuum oven at 60 °C for 24 h. Melt-mixing of PBS with OMMT was carried out using an internal mixer (Haake Poly-Drive R600, Germany). The mixing process was performed for 5 min at a temperature of 135 °C and a rotary speed of 50 rpm. After that, the compound was dried in a vacuum oven at 60 °C for 24 h. The dried compound was then molded on a compression molding machine (GoTech GT7014-A30C, Taiwan) into 1 mm sheets at 135 °C for 3 min. The specimens were subsequently prepared into a dumbbell shapes.

2.3. Moisture absorption

After molding, the samples were dried in a vacuum oven at 60 °C until a constant weight was reached. The moisture conditioning was performed in a Binder K720 Climatic Chamber (USA) at 30 °C, at 60% and 90% RH. For 100% RH, the samples were immersed in distilled water at 30 °C. Weight gains were determined by periodically removing the samples from their test environments, wiping them with a dry cloth and weighing them on a balance. The moisture absorption test was carried out for 60 days at each condition. The percentage of weight gain, M_t, at any time t as a result of moisture absorption was determined by the following equation:

$$M_t\ (\%) = \frac{W_w - W_d}{W_d} \times 100 \quad (1)$$

where W_d is the initial weight of the materials and W_w is the weight of the materials after exposure to the moisture. The equilibrium moisture content, M_m, was calculated as an average value of several consecutive measurements that showed no appreciable additional absorption. The diffusion coefficient, D, is given as [16]:

$$\frac{M_t}{M_m} = 1 - \frac{8}{\pi^2}\exp\left[-\left(\frac{Dt}{h^2}\right)\pi^2\right] \quad (2)$$

where h is the thickness of the sample.

2.4. Hygrothermal aging

Hygrothermal aging was carried out by the immersion of the samples in distilled water and placement in a water bath at different temperatures (30 °C, 60 °C and 80 °C). The weight change of the samples was determined by procedures similar to those used in the moisture absorption test. The physical changes of the samples were observed. Hygrothermal aging was performed for 60 days at 30 °C and 60 °C. At 80 °C, the test was carried out until all the samples fractured during the immersion.

2.5. Mechanical properties

Tensile properties were studied by using universal testing machine (Instron 3366, USA) at room temperature. Tensile testing was carried out according to the ASTM D638-03 (Type IV) standard with a gauge length of 50 mm and a cross-head speed of 5 mm/min. Five measurements were conducted on each sample.

2.6. Morphological properties

The tensile-fractured surface and the surface morphology of the samples were examined under a field-emission scanning electron microscope (FESEM) (Zeiss LEO Supra 35VP, Germany). Prior to the observations, the sample was sputter-coated with a thin layer of gold to avoid electrical charging during examination.

2.7. Thermal behavior

The thermal behavior of the nanocomposites was studied by differential scanning calorimetry (DSC) using a Perkin–Elmer DSC-6 (USA) in a nitrogen atmosphere. First, the sample was heated from 30 °C to 150 °C at a heating rate of 10 °C/min and held for 5 min at 150 °C. The sample was then cooled from 150 °C to 30 °C at the same heating rate and held for 5 min. The first heating cycle was done to eliminate the thermal history of the sample. After that, the second heating cycle was carried out from 30 °C to 150 °C. Finally, the sample was cooled to room temperature. The melting temperature (T_m), crystallization temperature (T_c) and degree of crystallinity (χ_c) were analyzed from the second scan. χ_c was calculated using the following equations [14]:

For pure PBS,

$$\chi_c = \frac{\Delta H_c}{\Delta H_m^0} \times 100\% \quad (3)$$

where ΔH_c = crystallization enthalpy of the sample.

ΔH_m^0 = melting enthalpy of 100% crystalline PBS (110.3 J/g).

For the polymer nanocomposites,

$$\chi_c = \frac{\Delta H_c}{\Delta H_m^0\left(1 - W_f\right)} \times 100\% \quad (4)$$

where W_f = weight fraction of fillers in the nanocomposite.

2.8. Degradation analysis

Degradation of the samples was investigated by Fourier transform infrared (FTIR) spectroscopy. The FTIR spectra were obtained on a Perkin–Elmer Spectrum One FTIR Spectrometer (USA) with the scanning wavelength from 4000 to 400 cm^{-1} and 32 scanning times. In addition, the pH of the distilled water after aging was determined using a CyberScan pH510 m (EUTECH Instruments, Singapore).

2.9. Molecular weight determination

The molecular weight of PBS was measured by gel permeation chromatography (GPC) analysis. GPC analysis was performed at 40 °C on an Agilent Technologies 1200 Series GPC system (USA) equipped with a refractive index detector (RID) and SHODEX K-806 M and SHODEX K-802 columns. The calibration of the columns was carried out using a polystyrene standard of known molecular weight and polydispersity. The samples were then dissolved in chloroform at ambient temperature, followed by filtration to eliminate the contaminants. Chloroform was used as the eluent

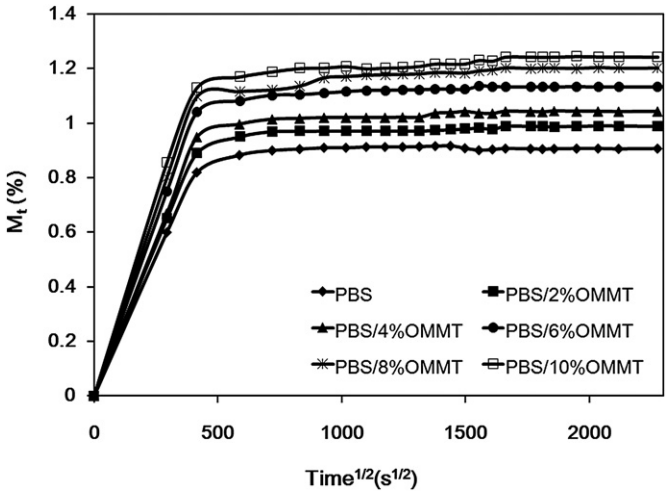

Fig. 1. Typical moisture uptake curves at 30 °C and 90% RH.

with a flow rate of 0.8 ml/min, and the injected sample volume was 50 μl with a polymer concentration of 1 mg/ml. The weight-average molecular weight (M_w) and number-average molecular weight (M_n) were obtained from the GPC analysis. The polydispersity index (PDI) was calculated as M_w/M_n [17]. The average number of random chain scissions per unit mass (n_t) can be calculated by [18–20]:

$$n_t = \frac{1}{M_n} - \frac{1}{M_{no}} \quad (5)$$

where M_{no} and M_n are the number-average molecular weight at zero and time t during aging, respectively.

3. Results and discussion

This section is divided into two parts. The first part discusses the effect of moisture absorption on PBS and its nanocomposites at different RH, and at a constant temperature of 30 °C. The second part is mainly focused on the effect of hygrothermal aging on PBS and its nanocomposites at different temperatures.

3.1. Moisture absorption at different relative humidity

3.1.1. Kinetics of moisture absorption

From the previous study, the effects of OMMT and RH on the moisture uptake have been reported [6] and thus will not be discussed in detail in this paper. The moisture uptake curves at 60, 90 and 100% RH exhibit the same trend as presented in Fig. 1.

In all conditions, the curves show a Fickian's behavior during the initial period of exposure, as revealed by the linear increment of moisture uptake with the square root of time [12,21]. After a certain period, the moisture uptake attained a steady state, at which M_m was reached. As discussed in the previous publication [6], the moisture uptake increased with the OMMT content and RH, which is verifiable by the M_m and D. This is attributed to the hydrophilic nature of the ODA groups, which acts as an intercalant in the OMMT, where they tend to interact with the water molecules by forming hydrogen bonds [11,22].

3.1.2. Mechanical properties

The tensile properties of PBS and its nanocomposites were investigated after 60 days of exposure to moisture at different RH. Before exposure to moisture, the optimum mechanical properties were observed in the PBS/2%OMMT nanocomposite. A further increment in the OMMT loading from 4 to 10 wt% reduced the mechanical properties due to agglomerations of OMMT in the PBS matrix [6]. From Table 1, it is interesting to note that the tensile strength of neat PBS increased after moisture absorption. This interesting effect arises as a result of the residual stress relaxation in the samples during moisture absorption. Residual stress (also known as internal stress) is a frozen-in stress that results from the uneven cooling rates over the cross section during molding process [23]. Moisture diffuses preferentially into the amorphous regions of the polymer [19,24], leading to the relaxation of molecular chains, which subsequently releases the residual stresses [25]. Thus, an exceptional increment in the tensile strength could be observed.

However, the presence of moisture has decreased the tensile strength of PBS/OMMT nanocomposites. A decrease in the tensile strength is an indication of a weak adhesion between the OMMT and the PBS matrix. The action of moisture has resulted in the partial disruption of the filler-matrix bonds and the formation of microcavities. These microcavities will act as stress concentrators,

Table 1
Tensile properties of PBS and PBS/OMMT nanocomposites after 60 days of moisture absorption at different RH.

Compound	Mechanical Properties	Before	Relative Humidity (% RH)					
			60		90		100	
			Wet	Redried	Wet	Redried	Wet	Redried
PBS	TS (MPa)	32.62	36.20 (+11.0)	35.53 [108.9]	36.31 (+11.3)	35.20 [107.9]	36.68 (+13.7)	34.53 [105.9]
	M (MPa)	589.1	532.4 (−9.6)	520.2 [88.3]	521.6 (−11.5)	507.9 [86.2]	517.6 (−12.1)	554.1 [94.1]
	E_b (%)	10.9	16.1 (+47.7)	13.3 [122.0]	16.2 (+48.6)	12.8 [117.4]	16.87 (+54.8)	9.9 [90.8]
PBS/2%OMMT	TS (MPa)	33.56	31.05 (−6.0)	31.56 [94.0]	31.17 (−7.1)	32.82 [97.8]	29.82 (−11.1)	32.46 [96.7]
	M (MPa)	631.8	554.8 (−12.2)	555.8 [88.0]	630.5 (−0.2)	631.7 [100.0]	609.2 (−3.6)	630.3 [99.8]
	E_b (%)	12.9	12.4 (−3.9)	8.5 [65.9]	12.2 (−3.9)	12.4 [96.1]	8.1 (−37.2)	9.1 [70.5]
PBS/4%OMMT	TS (MPa)	29.57	28.57 (−3.4)	28.77 [97.3]	28.41 (−3.9)	29.07 [98.3]	29.04 (−1.8)	29.26 [99.0]
	M (MPa)	685.8	592.7 (−13.6)	619.8 [90.4]	683.3 (−0.4)	684.6 [99.8]	627.2 (−8.5)	633.0 [92.3]
	E_b (%)	10.0	10.5 (+5.0)	10.3 [103.0]	10.2 (+2.0)	9.9 [99.0]	9.5 (−5.3)	6.0 [60.0]
PBS/6%OMMT	TS (MPa)	29.29	28.78 (−1.7)	29.54 [100.9]	27.06 (−7.6)	28.56 [97.5]	29.05 (−0.8)	29.11 [99.4]
	M (MPa)	714.8	641.6 (−10.2)	753.7 [105.4]	712.7 (−0.3)	713.4 [99.8]	652.9 (−8.7)	676.6 [94.7]
	E_b (%)	9.5	9.9 (+4.2)	9.7 [102.1]	9.5 (0.0)	9.4 [98.9]	9.2 (−3.2)	6.2 [65.3]
PBS/8%OMMT	TS (MPa)	26.86	26.09 (−2.9)	26.45 [98.5]	22.76 (−15.3)	23.46 [87.3]	24.04 (−10.5)	26.34 [105.5]
	M (MPa)	780.4	658.0 (−15.7)	731.3 [93.7]	778.3 (−0.3)	779.8 [99.9]	631.9 (−19.0)	744.4 [95.4]
	E_b (%)	9.4	9.6 (+2.1)	6.4 [68.1]	9.5 (+1.1)	9.4 [100.0]	6.5 (−30.9)	6.9 [73.4]
PBS/10%OMMT	TS (MPa)	26.09	24.11 (−7.6)	24.34 [93.3]	20.89 (−19.9)	22.56 [86.5]	19.87 (−23.8)	23.64 [90.6]
	M (MPa)	835.3	695.7 (−16.7)	793.7 [95.0]	828.5 (−0.8)	830.8 [99.5]	652.3 (−21.9)	764.9 [91.6]
	E_b (%)	8.9	9.3 (+4.3)	5.6 [62.9]	9.1 (+2.2)	9.0 [101.1]	4.64 (−47.9)	5.7 [64.0]

( ) Percentage of changes in the tensile properties after moisture absorption.
[ ] Percentage of recovery in tensile properties after re-drying.

which subsequently initiate matrix cracking and reduce both the stiffness and strength of nanocomposites [12,26,27]. The strength reduction is more significant at high RH due to the formation of more microcavities in an environment of high moisture content.

In addition, the presence of moisture generally reduced the modulus. This is mainly due to the plasticization effects induced by the absorbed moisture. After exposure, the microcavities were filled with water, which acts as a plasticizer to lower the stiffness [28]. Another reason for the plasticization is the formation of hydrogen bonds between water molecules and carbonyl groups [29] in PBS as proposed in Fig. 2. Furthermore, the tensile modulus decreased with the OMMT loading, owing to the formation of more microcavities at the filler-matrix interphase region.

The elongation at break for neat PBS increased with the RH. This indicates that moisture merely acts as a plasticizer in the polymer and subsequently softened the PBS. However, moisture-induced plasticization in PBS has further weakened the interfacial interactions between PBS and OMMT as mentioned earlier, causing a reduction in the elongation at break of PBS nanocomposites. These effects became more significant at 100% RH. Upon re-drying, both the strength and the modulus of the nanocomposites were recovered. However, the recovery of the elongation at break upon re-drying was rather limited.

3.1.3. Morphological properties

Figs. 3–5 show the tensile-fractured surfaces of neat PBS and PBS/OMMT nanocomposites. Before exposure to moisture, neat PBS exhibits a smooth fracture surface with some fibrils that form a web-like structure. However, upon exposure to moisture for 60 days at 100% RH, a rough surface with some microvoids was observed (Fig. 3b). The presence of moisture increased the matrix ductility and caused plasticization of PBS. This explains the increment in the elongation at break and the reduction in modulus. In addition, the formation of microvoids reveals the hydrolysis of PBS. This is in agreement with the studies of Kim and Kim [30], who reported on the degradation of PBS under high humidity condition for 30 days.

For PBS/2%OMMT nanocomposites, the clay platelets could not be observed clearly from the SEM micrograph as shown in Fig. 4a. This is attributed to the well-dispersed OMMT that forms intercalated and exfoliated structures in the PBS matrix. After 60 days of exposure to moisture, the surface becomes rougher due to plasticization. Furthermore, the detachment of the clay platelets from the PBS matrix by the formation of microcavities at the filler-matrix interphase is significant. These microcavities are the main reason for the decrease in the stiffness and strength [12].

The agglomeration of the OMMT is obvious in nanocomposites at high OMMT loading. Large clusters of OMMT could be seen in the PBS/10%OMMT nanocomposite under SEM (Fig. 5a). This is the main reason for the dramatic reduction in mechanical properties of nanocomposites beyond 2 wt% of OMMT loading. Furthermore, the increment in OMMT loading caused embrittlement of the nanocomposites. After exposure to moisture, the formation of large cavities at the filler-matrix interphase was more obvious (Fig. 5b).

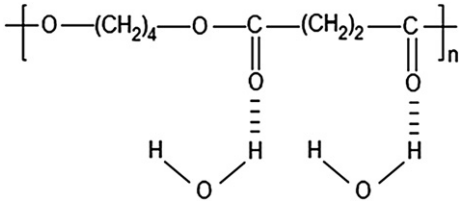

Fig. 2. Proposed interactions between water molecules and carbonyl groups in PBS.

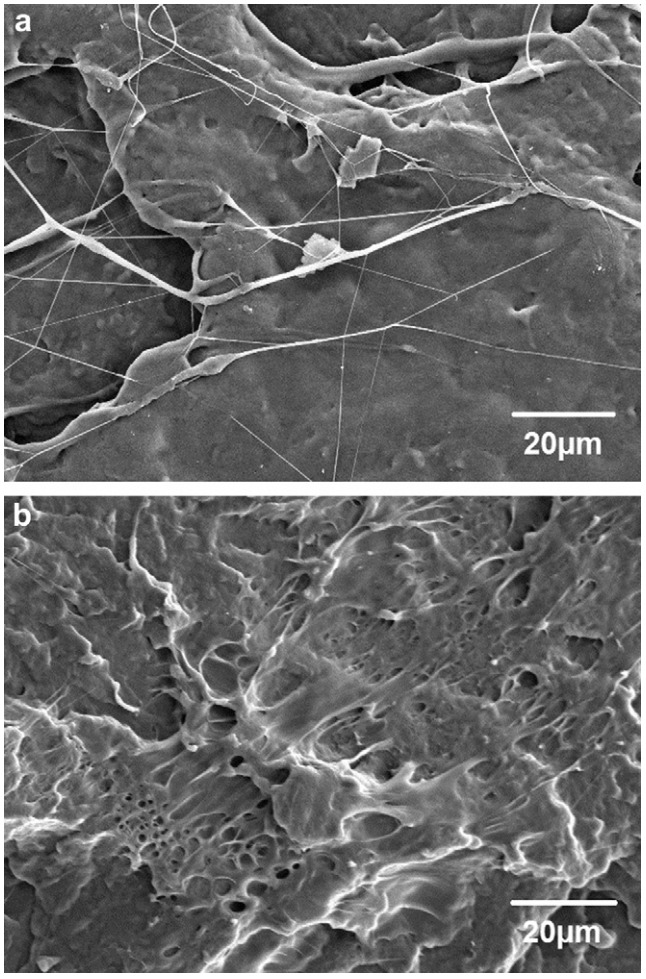

Fig. 3. SEM micrograph of the tensile-fractured surface of neat PBS (a) before and (b) after moisture absorption at 100% RH.

3.1.4. Thermal behavior

The thermal behavior of PBS and PBS/OMMT nanocomposites was investigated by differential scanning calorimetry (DSC) and is summarized in Table 2. Fig. 6 compares the DSC thermograms of neat PBS and PBS/OMMT nanocomposites during heating and cooling. Before exposure to moisture, two distinct endothermic peaks, i.e., '*x*' and '*z*', were found in both the PBS and its nanocomposites during heating. The lower melting endotherm '*x*' corresponds to the melting of the original crystals formed at the isothermal crystallization temperature, while the higher melting endotherm '*z*' indicates the melting of the crystals formed by the recrystallization process during the DSC analysis. A similar melting behavior of PBS has been reported by Qiu et al. [31] and Ray et al. [32]. In addition, an exothermic peak, which resulted from the fusion and recrystallization of PBS crystals during heating, was found for all the samples after the '*x*' endotherm [33].

After exposure to moisture, the endotherm '*x*' and '*z*' broadened. However, the variance in OMMT loading and RH did not notably change the $T_{m,x}$ and $T_{m,z}$. An additional melting endotherm (labeled as '*y*') is clearly seen in the PBS samples after moisture absorption. This endotherm corresponds to the formation of a different crystal lamella thickness under the influence of moisture. In the nanocomposites, the interaction between the PBS and the OMMT restricts the chain mobility and suppresses the recrystallization. Thus, endotherm '*y*' is absent in the heating scans of the nanocomposites.

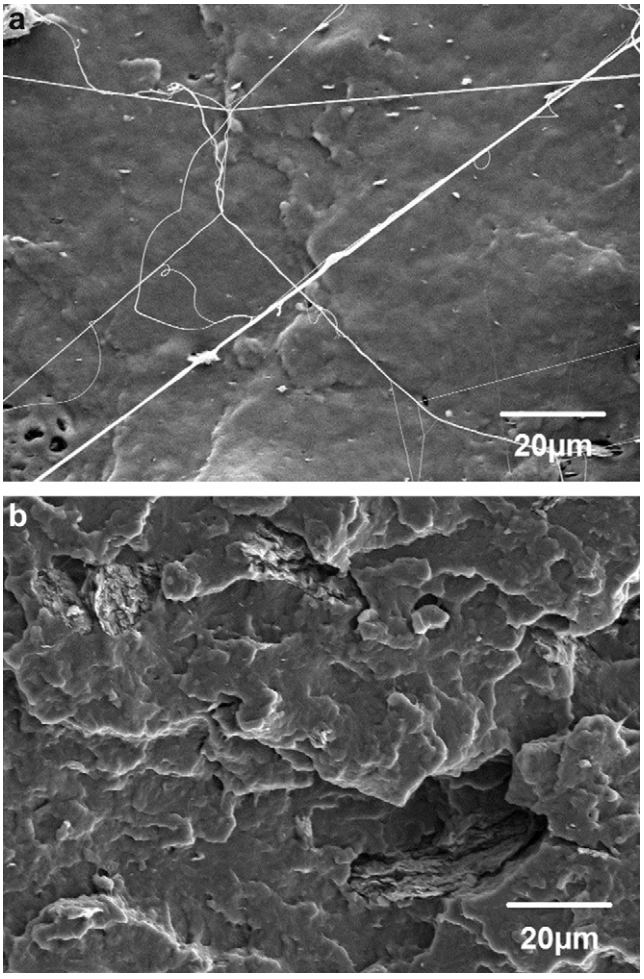

Fig. 4. SEM micrograph of the tensile-fractured surface of PBS/2%OMMT (a) before and (b) after moisture absorption at 100% RH.

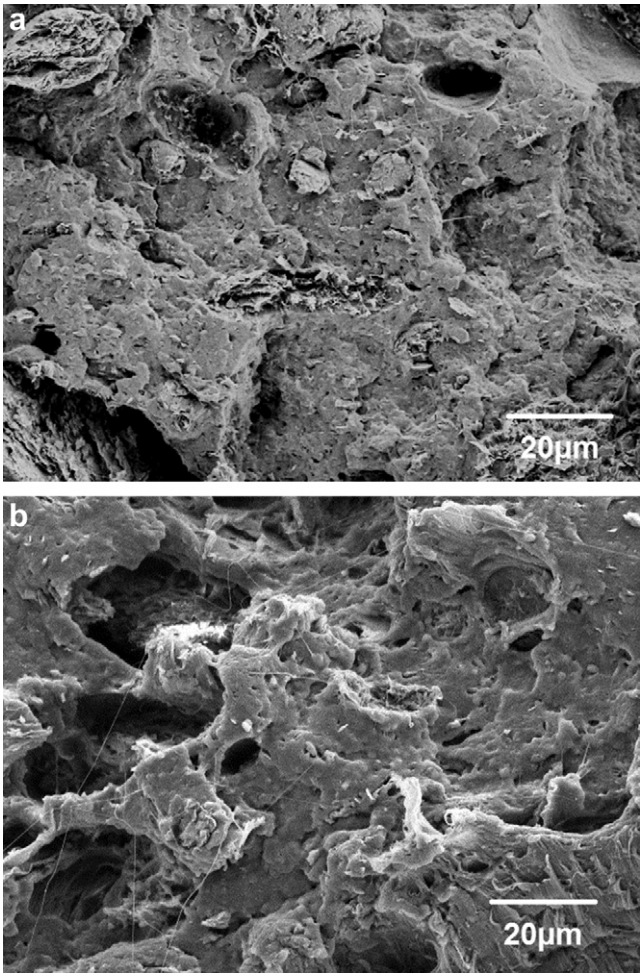

Fig. 5. SEM micrograph of the tensile-fractured surface of PBS/10%OMMT (a) before and (b) after moisture absorption at 100% RH.

The DSC cooling scans of PBS and PBS/2%OMMT are plotted in Fig. 6b. For neat PBS, χ_c decreases at 60% RH due to the penetration of moisture that restricts the recrystallization. However, χ_c was found to slightly increase at higher RH (90% and 100% RH). Some degree of hydrolytic degradation might occur during exposure to a more critical humid environment. The reduction in molecular weight generally favors the chain mobility and the ability of the chains to orient in an ordered structure or crystallize [19]. In the nanocomposites, the reduction of χ_c is significant at high RH and OMMT loading. The χ_c of PBS/10%OMMT decreased drastically after 60 days of exposure at 100% RH. This indicates that the interaction between water molecules and the ODA groups on the OMMT surface [34] further constrains the crystallization process. In addition, the OMMT platelets act as obstacles to the for mobility and flexibility of the polymer chains to fold and join the crystallization growth front [32]. This is also the reason for the lowering of T_c after moisture absorption in the PBS/OMMT nanocomposites.

3.2. Hygrothermal aging at different temperature

3.2.1. Moisture absorption and physical changes

Fig. 7a and b show the moisture absorption curves of PBS and its nanocomposites at immersion temperatures of 60 °C and 80 °C, respectively. Neither curves show a Fickian's behavior because constant saturation is not observed [12,35,36]. It reveals the occurrence of two kinetically distinct phenomena: moisture absorption that leads to the weight increment, and desorption of low molecular weight groups that reduces the sample weight [37]. The moisture uptake increased during the initial period of exposure and stopped after a short period followed by a gradual reduction. The weight loss mechanism can be attributed to either the chemical scission of the ester groups in PBS [11,30,38] or the diffusion of OMMT induced by cracks and leaching [37].

The moisture absorption curves at 60 °C show multiple steps of desorption. Cracking is noticeable on the samples (Fig. 8), which is associated with the desorption of degraded PBS and the leaching of

Table 2
DSC results for PBS and nanocomposites at different RH.

Compound	$T_{m,x}$ (°C)	$T_{m,y}$ (°C)	$T_{m,z}$ (°C)	T_c (°C)	χ_c (%)
PBS (before)	102.2	–	112.4	85.9	57.6
PBS (60%RH)	100.1	109.6	113.6	83.6	48.1
PBS (90%RH)	100.2	109.7	113.9	83.3	59.7
PBS (100%RH)	100.1	109.8	114.0	83.1	60.1
PBS/2%OMMT (before)	102.1	–	113.4	85.6	55.7
PBS/2%OMMT (60%RH)	104.0	–	114.6	80.2	50.4
PBS/2%OMMT (90%RH)	103.7	–	114.5	79.8	48.8
PBS/2%OMMT (100%RH)	100.8	–	115.0	79.3	47.5
PBS/10%OMMT (before)	102.2	–	113.3	85.5	55.9
PBS/10%OMMT (60%RH)	101.7	–	113.1	78.2	51.9
PBS/10%OMMT (90%RH)	103.4	–	114.2	79.9	45.9
PBS/10%OMMT (100%RH)	100.9	–	115.6	78.5	26.6

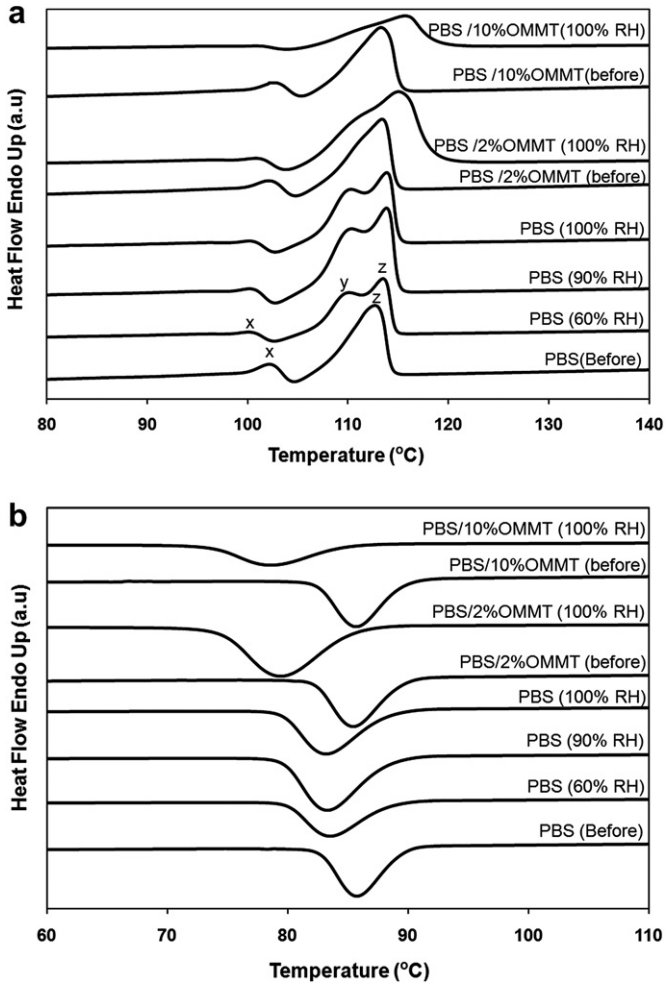

Fig. 6. DSC (a) heating scans and (b) cooling scans of PBS and nanocomposites at various RH and OMMT loadings.

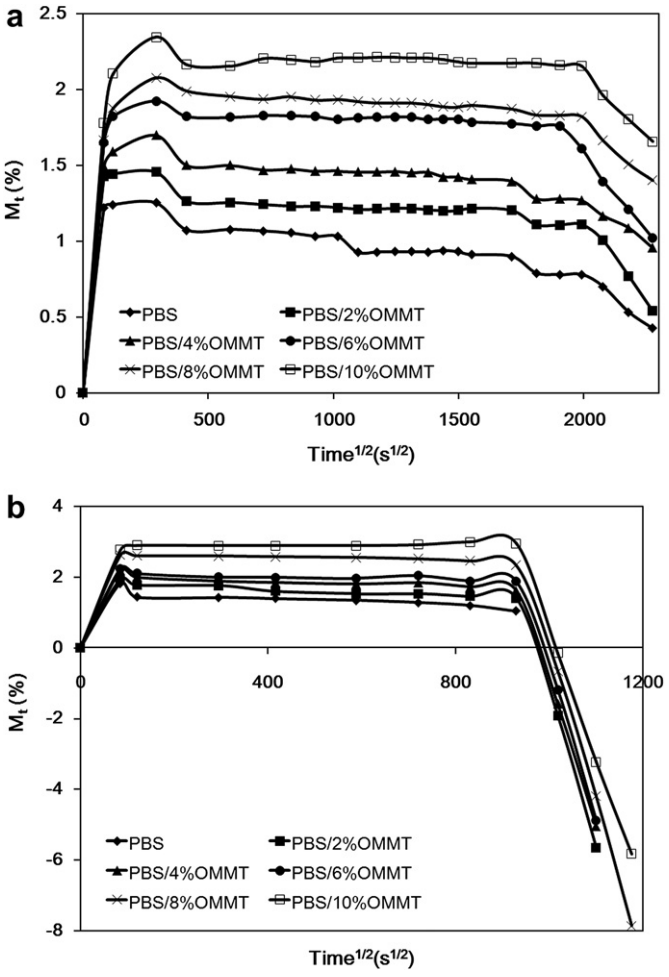

Fig. 7. Weight change during hygrothermal aging at (a) 60 °C and (b) 80 °C.

OMMT from the nanocomposites. From Fig. 7a, it could be observed that the neat PBS experienced more steps of desorption as compared to the nanocomposites. This indicates that hydrolytic degradation is more dominant in PBS due to a larger continuous phase of the polymer matrix. During hygrothermal aging, water molecules attack the ester groups in PBS, leading to the development of cracks with a simultaneous material loss. These cracks propagate throughout the matrix when higher material loss occurs. Moreover, the nanocomposites with high OMMT loading exhibit higher moisture uptake but less desorption. The presence of OMMT which acts as an obstacle is able to restrict the crack propagation in the matrix phase, subsequently constraining the desorption process.

The chemical scission of polymer chains is accelerated by increasing the immersion temperature. A dramatic desorption could be observed after 10 days of immersion at 80 °C (Fig. 7b). The samples became fragile and were unable to support external stress after exposure to moisture at 80 °C. Serious embrittlement occurred, leading to premature failure and fragmentation of the samples within a short time period. All the samples were fractured and fragmented within 16 days of immersion (Fig. 9). As seen in Fig. 7b, the neat PBS failed prior to the nanocomposites. As mentioned above, the addition of OMMT constrains the crack propagation. This is in agreement with the observation during hygrothermal aging at 60 °C.

3.2.2. Morphological properties

Fig. 10a–d display the surface morphologies of PBS after hygrothermal aging at different temperatures. PBS exhibits a relatively smooth and clear surface before exposure to moisture and

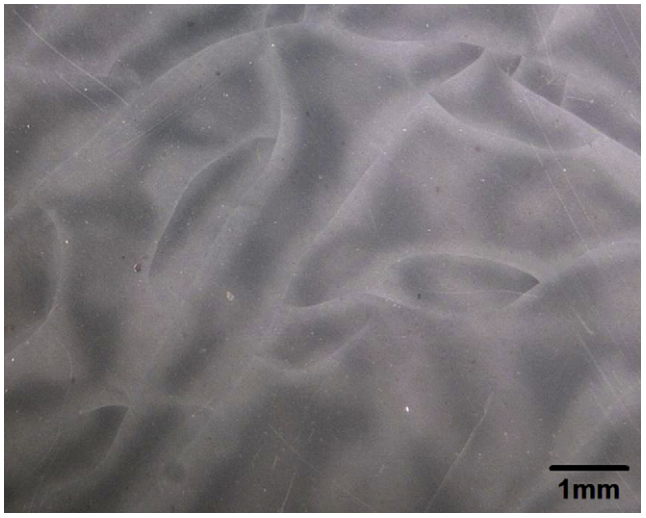

Fig. 8. The surface of PBS/2%OMMT nanocomposites observed by optical microscopy with 0.67x magnification after 60 days of hygrothermal aging at 60 °C.

Fig. 9. Premature failure and fragmentation of samples after 16 days of hygrothermal aging at 80 °C.

temperature. No notable change is observed in the surface morphology after 60 days of water absorption at 30 °C (Fig. 10b). However, at high immersion temperature, the degradation of PBS caused permanent damage to the material. Microcracks formed under hygrothermal aging at 60 °C and 80 °C. At 80 °C, visible erosion could be detected on the surface due to the extensive degradation of PBS at high temperature.

As mentioned earlier, the addition of OMMT into PBS matrix could act as an obstacle to restrict the crack propagation. This is verifiable via SEM as shown in Fig. 11. Short and non-continuous cracks, which were obstructed by the clay platelets, formed in the PBS/10%OMMT nanocomposites after hygrothermal aging at 80 °C. Furthermore, significant erosion can be observed on the sample surface.

3.2.3. Degradation analysis

An evaluation on the pH of the water before and after hygrothermal aging enables a qualitative determination on the extent of degradation. The pH decreases after hygrothermal aging as presented in Table 3. The degradation induces the formation of carboxyl (−COOH) end groups and subsequently yields an acidic environment. This finding is in agreement with that reported by Foulc et al. [20] and Blasi et al. [39]. It is noted that the pH of distilled water decreased with the immersion temperature, e.g., from 7.27 to 3.37 after aging of PBS at 80 °C. This confirms that the degradation is more extensive at higher temperature as discussed earlier. The reduction of the water pH value is more significant for the immersion of the nanocomposites as compared to the neat PBS. The leaching of amine groups from the OMMT surface into water might cause a reaction between amine groups and hydrogen ions (H^+) in water, producing a conjugate acid that contains NH^{4+}, which reduces the pH.

Fig. 12a shows the FTIR spectra of the PBS and the nanocomposite before and after the hygrothermal aging. The peak at 917 cm^{-1} results from the −C−OH bending in the carboxylic acid groups of PBS. The bands at 1044–1046 cm^{-1} were due to −O−C−C− stretching vibrations in PBS [15,40]. Peaks in the range of 1144–1264 cm^{-1} correspond to the stretching of the −C−O−C− group in the ester linkages of PBS. The peaks at 1330 cm^{-1} and 2945 cm^{-1} were assigned to the symmetric and asymmetric deformational vibrations of $-CH_2-$ groups in the PBS main chains, respectively.

Similar transmittance bands were observed in the PBS/2%OMMT nanocomposites as shown in Fig. 12b. The vibrations of the OMMT clay are shown at 1042 cm^{-1} (Si−O), 880 cm^{-1} (Al−O−H), and 800 cm^{-1} (Al−Mg−O−H) [41]. However, certain peaks overlapped

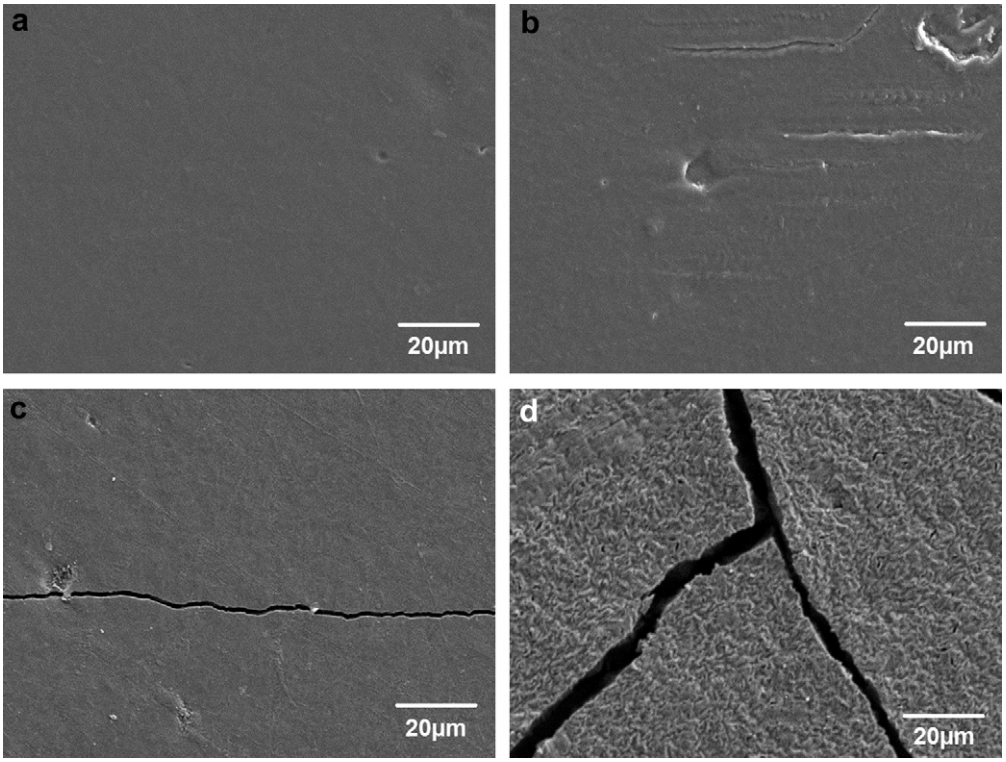

Fig. 10. SEM micrograph of the PBS surface (a) before and after exposure to water at (b) 30 °C, (c) 60 °C and (d) 80 °C.

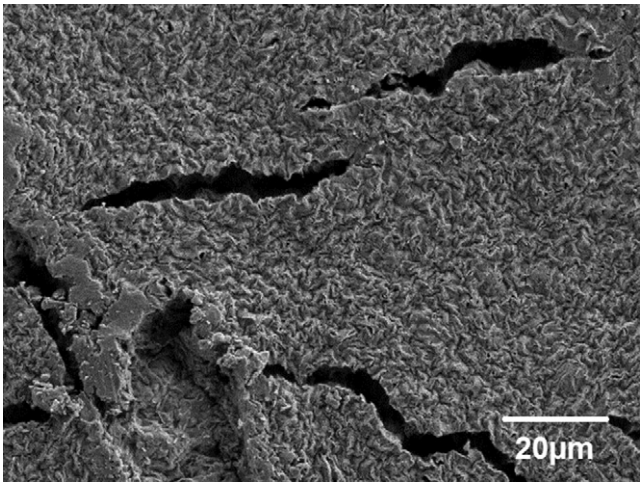

Fig. 11. SEM micrograph of the PBS/10%OMMT surface under hygrothermal aging at 80 °C for 16 days.

with the transmittance bands of the PBS matrix. Moreover, additional peaks at 3428 cm^{-1} ($-NH_2$) and 721–724 cm^{-1} ($-NHR$) in the nanocomposites were attributed to the stretching and deformation of the amine groups in ODA, which functioned as the intercalant in OMMT. After hygrothermal aging, a remarkable decrease in the transmittance intensity was observed. This results from the deterioration of the chemical structure and a lowering of molecular weight [42,43] of PBS after hygrothermal aging. Furthermore, an additional peak at 824 cm^{-1} was observed in PBS/2%OMMT which aged at 80 °C. This peak corresponds to the $-NH_2$ wag of the primary amines that were extracted from OMMT as a result of the hygrothermal aging.

3.2.4. Molecular weight determination

The measurement of molecular weight permits the quantitative determination of the extent of hydrolytic degradation. Table 4 reports the M_w and M_n of PBS before and after hygrothermal aging. The M_w of the PBS is given as 1.4×10^5 [44]. After the mixing and molding steps, the molecular weight was found to decrease as a result of chain breakage by shearing. After hygrothermal aging, a significant reduction in M_w and M_n was observed, confirming the occurrence of degradation caused by the hydrolysis of ester linkages in PBS [19]. The hydrolysis reaction can occur through two mechanisms: (i) random chain scission at ester linkages and, (ii) a depolymerization process. The molecular weight degradation is permanent damage caused by irreversible chemical mechanisms [12]. Moreover, it was found that greater hydrolytic degradation took place at high immersion temperature.

PDI is a measure of the distribution of molecular weight in a polymer. The decrease in PDI with decreasing temperature was observed. Higher temperature resulted in a rapid hydrolysis rate thus, homogenous hydrolysis is attained in a shorter time.

Table 3
pH values of water before and after hygrothermal aging.

Water After Immersion	Immersion Temperature (°C)	pH
Pure distilled water	–	7.27
PBS	30	7.19
	60	4.97
	80	3.37
PBS/2%OMMT	30	7.03
	60	4.03
	80	3.34

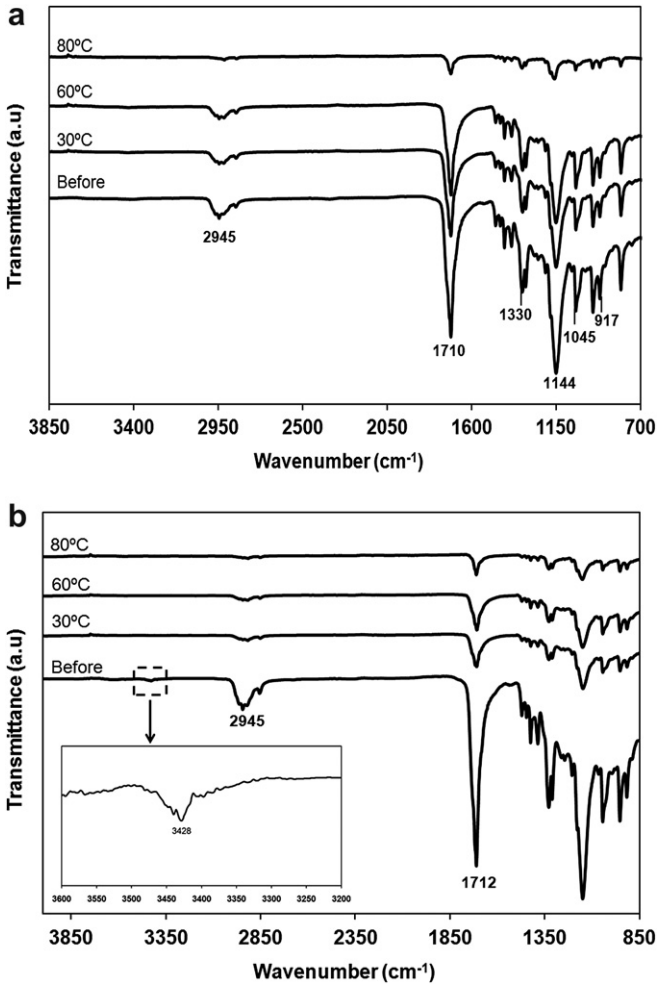

Fig. 12. FTIR Spectra of (a) PBS and (b) PBS/2%OMMT nanocomposites at various immersion temperatures and OMMT loadings.

Homogeneous hydrolysis brought about a narrow molecular weight distribution with a lower PDI, which corresponds to more uniform chain lengths [20,39]. Moreover, higher immersion temperature led to an increased number of chain scissions, which was manifested by the higher n_t when the immersion temperature increased.

3.2.5. Thermal behavior

Fig. 13 and Table 5 present the DSC results of PBS and its nanocomposites at various immersion temperatures. The previous discussion reported that an additional melting endotherm '*y*' was observed in neat PBS after exposure to moisture due to the formation of a different crystal lamella thickness. As seen in Fig. 13a, the melting endotherms '*x*', '*y*' and '*z*' have shifted to lower temperatures after hygrothermal aging and became more

Table 4
GPC results of PBS before and after hygrothermal aging.

Immersion Temperature	M_w (g/mol)	M_n (g/mol)	PDI	n_t (mol/g)
Before	42,130	21,170	1.90	–
30 °C	29,640	18,250	1.62	7.54×10^{-6}
60 °C	7756	5119	1.49	1.48×10^{-4}
80 °C	1884	1283	1.47	7.32×10^{-4}

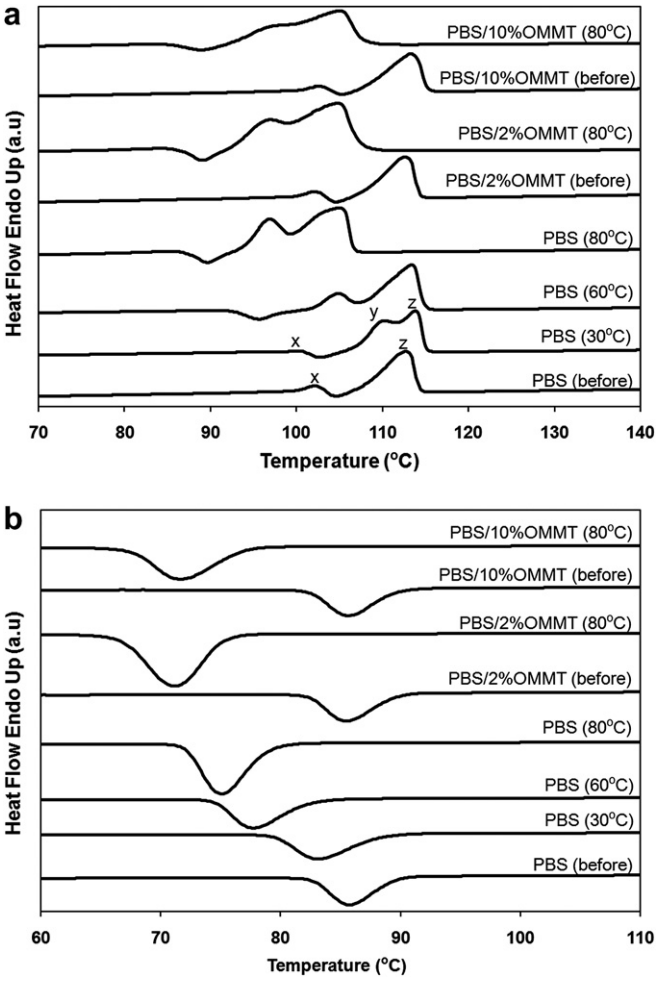

Fig. 13. DSC (a) heating scans and (b) cooling scans of PBS and the nanocomposites at various immersion temperatures and OMMT loadings.

promounced at high immersion temperature, i.e., at 80 °C. This is attributed to the hydrolytic degradation of PBS after aging [20]. Furthermore, the broadening of '*x*' indicates the destruction of the original crystal in PBS after aging. However, no notable change in the melting behavior was observed upon addition of the OMMT.

Table 5 shows that χ_c increased drastically with aging temperature. Crystallization is often favored by the reduction of molecular weight through chain scission during hygrothermal aging. Basically, chain scission might release the previously entangled chain segments in the amorphous phase. The shorter polymeric chains have a higher mobility and can rearrange into the crystalline phase. Pegoretti and Penati [19] reported this phenomenon as chemicrystallization, which is widely observed in biodegradable semicrystalline aliphatic polyesters, such as PBS. At 80 °C, a greater extent of chain scission led to a greater increase in χ_c. On the other hand, the increase in χ_c is slightly lower at high OMMT loading, owing to the restriction of the crystallization process by the OMMT platelets [32]. However, T_c decreased after aging. Chain scission allowed more polymer chains to be arranged in an ordered structure (i.e., to crystallize). Thus, the crystallization rate decreased because more time is needed for these chains to align.

Table 5
DSC results for PBS and PBS/OMMT nanocomposites at different immersion temperatures.

Compound	$T_{m,x}$ (°C)	$T_{m,y}$ (°C)	$T_{m,z}$ (°C)	T_c (°C)	χ_c (%)
PBS (before)	102.2	–	112.4	85.8	57.6
PBS (30 °C)	100.1	109.8	114.0	83.1	60.1
PBS (60 °C)	90.4	104.8	113.5	77.8	68.5
PBS (80 °C)	85.2	96.7	105.2	75.0	79.1
PBS/2%OMMT (before)	102.1	–	113.4	85.6	55.7
PBS/2%OMMT (30 °C)	100.8	–	115.0	79.3	47.5
PBS/2%OMMT (60 °C)	98.1	104.4	113.2	74.9	68.9
PBS/2%OMMT (80 °C)	84.3	96.3	104.9	71.3	74.9
PBS/10%OMMT (before)	102.2	–	113.3	85.5	55.9
PBS/10%OMMT (30 °C)	100.9	–	115.6	78.5	26.6
PBS/10%OMMT (60 °C)	89.1	104.2	113.3	73.5	71.7
PBS/10%OMMT (80 °C)	83.5	96.9	105.3	71.7	71.9

4. Conclusions

The incorporation of OMMT into PBS increased the moisture uptake. The mechanical properties of PBS nanocomposites, such as tensile strength and modulus decreased after exposure to moisture and heat. This was due to poor matrix-filler adhesion and microcavity formation. The lowering of the modulus also arose from the plasticization effect in the PBS matrix after exposure to moisture. Moreover, the increase in RH caused a reduction in the elongation at break of the nanocomposites. These effects became more pronounced at high RH and high temperature. At 80 °C, significant hydrolytic degradation occurred, which led to the premature failure of the material. This was verifiable via SEM, FTIR and GPC. The molecular weight of PBS clearly decreased after hygrothermal aging. From the DSC analysis, an additional peak was found after moisture absorption and hygrothermal aging. Hygrothermal aging lowered the T_m of the PBS nanocomposites with increasing immersion temperature, while the T_c decreased after moisture absorption and hygrothermal aging. The χ_c of PBS nanocomposites decreased with the RH at 30 °C. The interaction between water molecules and the ODA groups on the OMMT surface further constrained the crystallization of the nanocomposites at 30 °C. Upon immersion at 60 °C and 80 °C, χ_c increased drastically as a result of chain scission, which favors crystallization.

Acknowledgments

The financial support of USM Research University Grant (1001.PBAHAN.814016), USM Incentive Grant (1001.PBAHAN.8021011) and USM Fellowship is gratefully acknowledged. Technical support from Dr. Sudesh Kumar of the School of Biological Sciences, USM is also appreciated.

References

[1] Yoo ES, Im SS. Melting behavior of poly(butylene succinate) during heating scan by DSC. J Polym Sci, Part B: Polym Phys 1999;37(13):1357–66.
[2] Okamoto K, Ray SS, Okamoto M. New poly(butylene succinate)/layered silicate nanocomposites. II. effect of organically modified layered silicates on structure, properties, melt rheology, and biodegradability. J Polym Sci, Part B: Polym Phys 2003;41(24):3160–72.
[3] Chen GX, Kim ES, Yoon JS. Poly(butylene succinate)/twice functionalized organoclay nanocomposites: preparation, characterization, and properties. J Appl Polym Sci 2005;98(4):1727–32.
[4] Someya Y, Nakazato T, Teramoto N, Shibata M. Thermal and mechanical properties of poly(butylene succinate) nanocomposites with various organo-modifies montmorillonites. J Appl Polym Sci 2003;91(3):1463–75.
[5] Shih YF, Wang TY, Jeng RJ, Wu JY, Teng CC. Biodegradable nanocomposites based on poly(butylene succinate)/organoclay. J Polym Environ 2007;15(2):151–8.
[6] Phua YJ, Chow WS, Mohd Ishak ZA. Poly(butylene succinate)/organo-montmorillonite nanocomposites: effects of the organoclay content on mechanical, thermal and moisture absorption properties. J Thermoplast Compos Mater 2010;24:133–51.
[7] Phua YJ, Chow WS, Mohd Ishak ZA. Mechanical properties and structure development in poly(butylene succinate)/organo-montmorillonite nanocomposites under uniaxial cold rolling. eXPRESS Polym Lett 2011;5(2):93–103.

[8] Lee WK, Gardella Jr Joseph A. Hydrolytic kinetics of biodegradable polyester monolayers. Langmuir 2000;16(7):3401–6.
[9] Herzog K, Müller RJ, Deckwer WD. Mechanism and kinetics of the enzymatic hydrolysis of polyester nanoparticles by lipases. Polym Degrad Stab 2006; 91(10):2486–98.
[10] Pavlidou S, Papaspyrides CD. The effect of hygrothermal history on water sorption and interlaminar shear strength of glass/polyester composites with different interfacial strength. Composites Part A 2003;34(11):1117–24.
[11] Correlo VM, Pinhp ED, Pashkuleva I, Bhattacharya M, Neves NM, Reis RL. Water absorption characteristics of chitosan-based polyesters and hydroxy-apatite composites. Macromol Biosci 2007;7(3):354–63.
[12] Mohd Ishak ZA, Berry JP. Hygrothermal aging studies of short carbon fiber reinforced nylon 6.6. J Appl Polym Sci 1994;51(13):2145–55.
[13] Kim H, Yang H, Kim H. Biodegradability and mechanical properties of agro-flour-filled polybutylene succinate biocomposites. J Appl Polym Sci 2005; 97(4):1513–21.
[14] Zhao J, Wang X, Zeng J, Yang G, Shi F, Yan Q. Biodegradation of poly(butylene succinate) in compost. J Appl Polym Sci 2005;97(6):2273–8.
[15] Kim H, Kim H, Lee J, Choi I. Biodegradability of bio-flour filled biodegradable poly(butylene succinate) bio-composites in natural and compost soil. Polym Degrad Stab 2006;91(5):1117–27.
[16] Mohd Ishak ZA, Ishiaku US, Karger-Kocsis J. Hygrothermal aging and fracture behavior of short-glass-fiber-reinforced rubber-toughened poly(butylene terephthalate) composites. Compos Sci Technol 2000;60(6):803–15.
[17] Rogošić M, Mencer HJ, Gomzi Z. Polydispersity index and molecular weight distributions of polymers. Eur Polym J 1996;32(11):1337–44.
[18] Bellenger V, Ganem M, Mortaigne B, Verdu J. Lifetime prediction in the hydrolytic ageing of polyesters. Polym Degrad Stab 1995;49(1):91–7.
[19] Pegoretti A, Penati A. Recycled poly(ethylene terephthalate) and its short glass fibres composites: effects of hygrothermal aging on the thermo-mechanical behaviour. Polymer 2004;45(23):7995–8004.
[20] Foulc MP, Bergeret A, Ferry L, Ienny P, Crespy A. Study of hygrothermal ageing of glass fibre reinforced PET composites. Polym Degrad Stab 2005;89(3): 461–70.
[21] Panthapulakkal S, Sain M. Studies on the water absorption properties of short hemp-glass fiber hybrid polypropylene composites. J Compos Mater 2007; 41(15):1871–83.
[22] Kusmono, Mohd Ishak ZA, Chow WS, Takeichi T, Rochmadi. Water absorption behavior of different types of organophilic montmorillonite-filled polyamide 6/polypropylene nanocomposites. Polym Compos 2009;31(2):195–202.
[23] Rosato DV, Schott NR. Plastics engineering, manufacturing & data handbook. London: Kluwer Academic; 2001. 1559–1560.
[24] Launay A, Thominette F, Verdu J. Hydrolysis of poly(ethylene terephthalate)—a kinetic study. Polym Degrad Stab 1994;46(3):319–24.
[25] Vinson JR. Advanced composite materials—environmental effects. USA: ASTM International; 1978. 205–220.
[26] Athijayamani A, Thiruchitrambalam M, Natarajan U, Pazhanivel B. Effect of moisture absorption on the mechanical properties of randomly oriented natural fibers/polyester hybrid composite. Mater Sci Eng A 2009;517(1–2):344–53.
[27] Vlasveld DPN, Groenewold J, Bersee HEN, Picken SJ. Moisture absorption in polyamide-6 silicate nanocomposites and its influence on the mechanical properties. Polymer 2005;46(26):12567–76.
[28] Huang G, Sun H. Effect of water absorption on the mechanical properties of glass/polyester composites. Mater Des 2007;28(5):1647–50.
[29] Mikhaylova Y, Adam G, Häussler L, Eichhorn KJ, Voit B. Temperature-dependent FTIR spectroscopic and thermoanalytic studies of hydrogen bonding of hydroxyl (phenolic group) terminated hyperbranched aromatic polyesters. J Mol Struct 2006;788(1–3):80–8.
[30] Kim HS, Kim HJ. Enhanced hydrolysis resistance of biodegradable polymers and bio-composites. Polym Degrad Stab 2008;93(8):1544–53.
[31] Qiu Z, Ikehara T, Nishi T. Poly(hydroxybutyrate)/poly(butylene succinate) blends: miscibility and nonisothermal crystallization. Polymer 2003;44(8): 2503–8.
[32] Ray SS, Bousmina M, Okamoto K. Structure and properties of nanocomposites based on poly(butylene succinate-co-adipate) and organically modified montmorillonite. Macromol Mater Eng 2005;290(8):759–68.
[33] Pang MZ, Qiao JJ, Jiao J, Wang SJ, Xiao M, Meng YZ. Miscibility and properties of completely biodegradable blends of poly(propylene carbonate) and poly(butylene succinate). J Appl Polym Sci 2008;107(5):2854–60.
[34] Chow WS. Water absorption of epoxy/glass fiber/organo-montmorillonite nanocomposites. eXPRESS Polym Lett 2007;1(2):104–8.
[35] Li Y, Miranda J, Sue H. Hygrothermal diffusion behavior in bismaleimide resin. Polymer 2001;42(18):7791–9.
[36] Bao L, Yee AF, Lee CYC. Moisture absorption and hygrothermal aging in a bismaleimide resin. Polymer 2001;42(17):7327–33.
[37] Sobrinho LL, Ferreira M, Bastian FL. The effects of water absorption on an ester vinyl resin system. Mater Res 2009;12(3):353–61.
[38] Pepić D, Radoičić M, Nikolić MS, Djonlagić J. The influence of antioxidant and post-synthetic treatment on the properties of biodegradable poly(butylene succinate)s modified with poly(propylene oxide). J Serb Chem Soc 2007; 72(12):1515–31.
[39] Blasi P, Souza SSD, Selmin F, DeLuca PP. Plasticizing effect of water on poly(lactide-co-glycolide). J Control Release 2005;108(1):1–9.
[40] Pamuła E, Błażewicz M, Paluszkiewicz C, Dobrzyński P. FTIR study of degradation products of aliphatic polesters carbon fibers composites. J Mol Struct 2001;596(1–3):69–75.
[41] Wang M, Zhao F, Guo Z, Dong S. Poly(vinylidene fluoride-hexafluoropropylene)/organo-montmorillonite clays nanocomposite lithium polymer electrolytes. Electrochim Acta 2004;49(21):3595–602.
[42] Fanconi B. Molecular vibrations of polymers. Ann Rev Phys Chem 1980;31: 265–91.
[43] Berthé V, Ferry L, Bénézet JC, Bergeret A. Ageing of different biodegradable polyesters blends mechanical and hygrothermal behavior. Polym Degrad Stab 2010;95:262–9.
[44] Teeraphatpornchai T, Nakajima-Kambe T, Shigeno-Akutsu Y, Nakayama M, Nomura N, Nakahara T, et al. Isolation and characterization of a bacterium that degrades various polyester-based biodegradable plastics. Biotechnol Lett 2003;25(1):23–8.